

SIZE DEPENDENT MELTING BEHAVIOR OF Rh NANOPARTICLES BY MOLECULAR DYNAMICS SIMULATION

Unal DOMEKELI¹, Murat CELTEK², Sedat SENGUL¹

¹ Department of Physics, Faculty of Science, University of Trakya, 22030, Edirne, TURKEY

² Faculty of Education, University of Trakya, 22030, Edirne, TURKEY

Abstract

We have investigated size dependent the melting behavior of Rhodium (Rh) nanoparticles by using molecular dynamics simulations. The melting points of nanoparticles were estimated by following the changes in the total energy, heat capacity and pair distribution function. We observed that the melting temperature obtained from the molecular dynamics simulations increases as the particle size increases. Furthermore, the melting temperature of all nanoparticles is lower than that of bulk Rh. The melting temperatures of nanoparticles were also compared with the results of a theoretical model. The melting temperatures of the nanoparticles obtained from both methods are compatible with each other.

Keywords: Rh nanoparticle, MD simulation, melting temperature.

INTRODUCTION

It has been a great interest for researchers, as the novel melting behavior of metal nanoparticles has led to the development of new properties of materials with wide application areas [1-3]. Size dependent melting behavior of metallic nanoparticles can be examined by using three different methods: experimental [4,5], theoretical [6-8] and molecular dynamics (MD) simulation method [9-12]. Although there are some difficulties in analyzing the melting process of metal nanoparticles with experimental method, MD simulation provides a powerful method to investigate the structural and dynamic properties of nanoparticles and to obtain the related data. Therefore, size dependent the melting process of metallic nanoparticles having unique mechanical, optical, magnetic, electronic and catalytic properties is studied extensively by many researchers using the MD simulation technique.

As far as we know, the size-dependent melting behavior of Rh nanoparticles with good catalytic properties has not been investigated using this technique. In this study, we have investigated the size effect on melting behavior of Rh nanoparticles (NP) by using

MD simulations based on the quantum Sutton – Chen (QSC) potential [12,13].

EXPOSITION

In this study, MD simulations using DLPOLY [14] code have been performed to gain insights into the thermal properties of NPs at the atomic scale. Sutton-Chen potential was used to describe interactions between atoms in MD simulations. Based on the Sutton-Chen (SC) potential, the total potential energy of a finite system with N atoms is written as [12]

$$U_{tot} = \sum_i U_i, \quad (1)$$

$$U_i = \sum_i \varepsilon \left[\sum_{j \neq i} \frac{1}{2} V(r_{ij}) - c \rho_i^{1/2} \right], \quad (2)$$

where $V(r_{ij})$ is a pair potential between atoms i and j separated by the distance of r_{ij} to account for the repulsion resulting from Pauli's exclusion principle and ρ_i is a energy density term accounting for cohesion associated with atom i ,

$$V(r_{ij}) = \left(\frac{a}{r_{ij}} \right)^n, \quad (3)$$

$$\rho_i = \sum_{j \neq i} \varphi(r_{ij}) = \sum_{j \neq i} \left(\frac{a}{r_{ij}} \right)^m. \quad (4)$$

where the a is a parameter with the dimension of length leading to dimensionless $V(r_{ij})$ and ρ_i , c is a dimensionless parameter, ε is a parameter with the dimension of energy, and n and m are positive integers providing that $n > m$. The behavior of the total energy of the system at higher temperatures requires testing of the interatomic pair potentials used in the simulations. The QSC potential developed by Cagin et al. [13] is an improved potential of SC, which permits better estimation of temperature-dependent properties in the same way as the SC potential. We use the QSC potential which its parameters are listed in Table 1, to describe interatomic interactions.

Table 1. QSC potential parameters for Rh [13]

Metal	ε (eV)	c	a (Å)	n	m
Rh	3.4612×10^{-3}	305.499	3.7984	13	5

In order to investigate the size effects on melting temperature of Rh NPs, we constructed five NP consisting of 610, 1048, 2454, 4874 and 8272 atoms, representing the diameter of NPs ranging from 2.5 to 6 nm. All NPs were extracted from a large crystal structure of the ideal *fcc* Rh using a series of spherical cutoffs. MD simulations were performed using two different canonical ensembles. The nanoparticles were simulated under constant volume and constant temperature NVT ensemble without the periodic boundary conditions. For bulk system, we performed molecular dynamics under constant temperature and constant pressure NPT ensemble with a periodic boundary conditions. The stable structure at 0 K was obtained through the initial configurations annealed fully at $T=300$ K and then cooled to $T=0$ K at a cooling rate of 0.05 K/ps. The annealed configuration is almost the same as its initial configuration except for the relaxed surface atoms. For each NPs, the system was treated to the heating process consisting of a series of MD simulations with the temperature increment of $\Delta T=50$ K. The simulations were carried out for 100 ps of equilibration followed by production time of 50 ps for generating time-averaged properties at each temperature. The Newtonian equations

of motion are integrated using the Leapfrog Verlet method with a time step of 1fs. The desired temperature and ambient pressure are controlled by Nose- Hoover thermostat and Berendsen approach, respectively.

In the results section, we first discuss the quantities which may be used to single out the melting transition. One of the simplest ways to determine the melting point of the NP and bulk system in MD simulations is to monitor the change in the total energy curve of the system with temperature. The temperature-dependent changes of total energies of Rh nanoparticles and bulk system are shown in Figure 1.

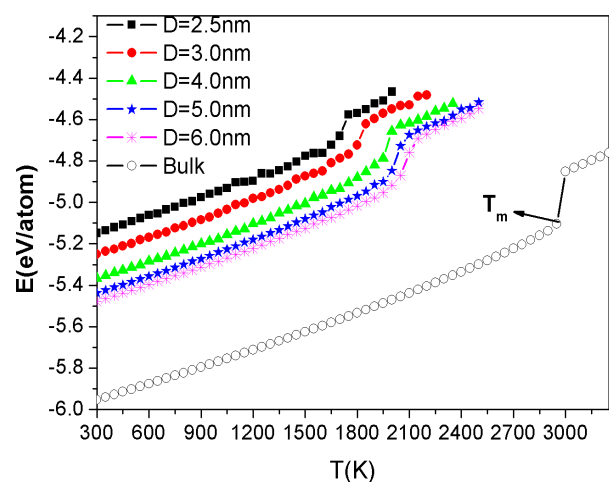


Fig. 1. Temperature dependence of the total energy for nanoparticles and bulk system

The total energies of the Rh nanoparticles were higher than that of bulk, because of increased surface energy as the size of the nanoparticle decreases. In addition, the total energy increased linearly with increasing temperature and suddenly changed near the melting point. The melting point is clearly defined by the sudden increase in total energy. The temperature values corresponding to the sudden change observed in total energy is defined as the melting temperature. The melting temperatures of all nanoparticles were lower than the melting temperature of the bulk Rh. Another way to determine the melting point by utilizing the thermodynamic properties of a system is to calculate the heat capacity. To calculate the heat capacity [15], we fitted smooth cubic splines to the average potential energy during the heating process as

a function of temperature and then obtained the derivative from this fitted curve,

$$C_p(T) = \frac{dE_p}{dT} + \frac{3R}{2} \quad (5)$$

where, E_p is the potential energy and R is the gas constant. To identify the melting point, the heat capacity C_p was plotted for all nanoparticles and bulk in Figure 2.

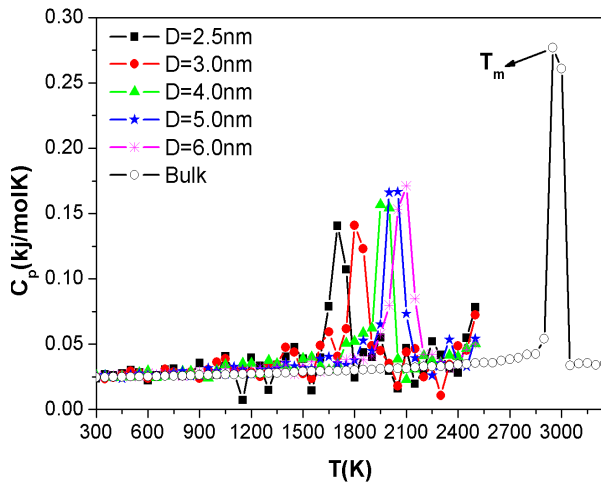


Fig. 2. Temperature dependence of heat capacity for nanoparticles and bulk system

The heat capacity has sharp peaks at the melting point due to latent heat. The temperature value corresponding to the maximum heat capacity corresponds to the temperature value at which the sudden change in potential energy is observed. This temperature value corresponds to the melting point of the system where the phase transition of the first-order occurs. Thus, the melting point of the system can easily be determined by the temperature dependent change behavior of the pair distribution function. It is defined as:

$$g(r) = \frac{\Omega}{N^2} \langle (\sum_{i=1}^{N_i} n_i) / 4\pi r^2 \Delta r \rangle \quad (6)$$

where, $g(r)$ is the probability of finding an atom in a distance ranging from r to $r+\Delta r$. Ω is simulated volume of unit cell. N is the number of atoms in the systems, and N_i is the averaged number atom around i th atoms sphere shell ranging r to $r+\Delta r$, where Δr is the step of calculation. Figure 3 shows the pair distribution function of nanoparticle with a diameter of $D=5\text{nm}$ range between 300 and 2050K during heating process.

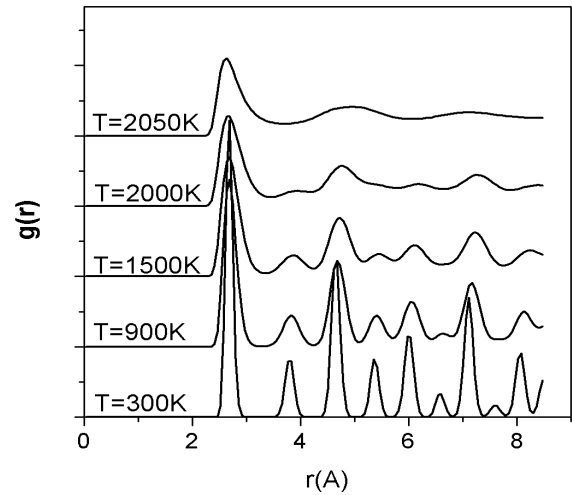


Fig. 3. Temperature dependence of the pair distribution functions of nanoparticle with a diameter of $D=5\text{nm}$ during heating

As can be seen from Figure 3, the characteristic behavior of the pair distribution function of the nanoparticle at 300K explains that the nanoparticle has an ideal *fcc* structure. As high temperatures are reached, the peak widths of pair distribution function increase while peak amplitudes decrease. The nanoparticle's pair distribution function exhibits solid state behavior in the 300-2000K temperature range, while exhibiting a liquid state at 2050K. This shows that the nanoparticle began to melt in 2000K and the system is completely liquid at 2050K. The size-related variation of the melting temperatures obtained from MD simulation for Rh nanoparticles is shown in Figure 4.

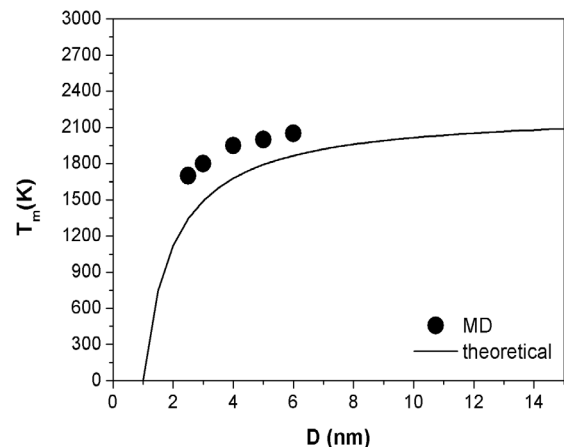


Fig. 4. Variation of the melting temperature of Rh nanoparticles depending on particle diameter

Also, the melting temperatures for Rh NPs were calculated using the liquid drop model given by Nanda et al [6]. The melting

temperatures, calculated by using theoretical model were compared with MD results in Figure 4. As the particle size increases, the melting temperatures of the nanoparticles increase. This increase in melting temperature is faster in small sizes, but is slower in large sizes.

CONCLUSION

In this work, the size dependent melting behaviors of Rh nanoparticles have been investigated by the molecular dynamics simulation using QSC potential. The results are revealed that the melting temperatures of the Rh nanoparticles obtained from both models are consistent with each other and lower than the melting temperature of the bulk Rh. The melting temperature of the Rh nanoparticles is also reduced by decreasing the particle diameter due to increased surface energy. This indicates that the unstable surface of free-standing nanoparticles leads to a reduction in the melting temperature.

REFERENCE

- [1] M. Zhao, Q. Jiang, *Solid State Commun.* 130, 37 (2004).
- [2] S.C. Tjong, H. Chen, *Mater. Sci. Eng. R.* 45, 1 (2004).
- [3] Q.S. Mei, K. Lu, *Prog. Mater. Sci.* 52, 1175 (2007).
- [4] P. Buffat, J. P. Borel, *Phys. Rev. A* 13, 2287 (1976).
- [5] K. F. Peters, J. B. Cohen, and Y. W. Chung, *Phys. Rev. B* 57, 13430-13438 (1998).
- [6] K. K. Nanda, S. N. Sahu, and S. N. Behera, *Phys. Rev. A* 66, 013208 (2002).
- [7] K. K. Nanda, *Pramana-J. Phys* 72, 617-628 (2009).
- [8] H. M. Lu, P. Y. Li, Z. H. Cao, X. K. Meng, *J. Phys. Chem. C* 113, 7598 (2009).
- [9] S. Alavi, D. L. Thompson, *J. Phys. Chem. A* 110, 1518–1523 (2006).
- [10] Q. Zhiwei, F. Haijun, Z. Jian, *Phase Transitions* 87, 59-70 (2014).
- [11] F. Delogu, *Rev. B* 72, 205418 (2005).
- [12] A.P. Sutton and J. Chen, *Philos. Mag. Lett.* 61, 139–146 (1990).
- [13] T. C□agin, Y. Qi, H. Li, Y. Kimura, H. Ikeda, W. L. Jonhson, and W. A. Goddard III, *MRS Symp. Ser.* 554, 43 (1999).
- [14] W. Smith and T. R. Forester, *J. Mol. Graphics* 14, 136 (1996).
- [15] U. Domekeli, S. Sengul, M. Celtek and C. Canan, *Philos. Mag. Lett.* 98, 371–387 (2018).